JGR Space Physics

RESEARCH ARTICLE
10.1029/2024JA032865

Estimating the Possible Ion Heating Caused by Alfvén Waves at Venus

G. Stenberg Wieser[1,2], M. André[3], H. Nilsson[1], N. Edberg[3], M. Persson[3], S. Rojas Mata[1], M. Mihalikova[4], H. Gunell[2], A. Bader[5], and Y. Futaana[1]

[1]Swedish Institute of Space Physics, Kiruna, Sweden, [2]Department of Physics, Umeå University, Umeå, Sweden, [3]Swedish Institute of Space Physics, Uppsala, Sweden, [4]EISCAT Headquarters, Kiruna, Sweden, [5]Gorillini NV, Antwerp, Belgium

Key Points:

- Energization of O^+ escaping from Venus by Alfvén waves to keV energies is plausible
- The estimated electric power spectral density at the typical oxygen gyrofrequency is in the range 0.5–10 $(mV/m)^2/Hz$ close to the planet
- An estimated heating rate of ≈3 eV/s is enough to explain oxygen thermal energies up to a keV

Correspondence to:

G. Stenberg Wieser,
gabriella.stenberg.wieser@irf.se

Citation:

Stenberg Wieser, G., André, M., Nilsson, H., Edberg, N., Persson, M., Rojas Mata, S., et al. (2024). Estimating the possible ion heating caused by Alfvén waves at Venus. *Journal of Geophysical Research: Space Physics*, *129*, e2024JA032865. https://doi.org/10.1029/2024JA032865

Received 28 MAY 2024
Accepted 23 NOV 2024

Author Contributions:

Conceptualization: G. Stenberg Wieser, M. André, H. Nilsson
Formal analysis: G. Stenberg Wieser, H. Nilsson
Methodology: G. Stenberg Wieser, M. André, H. Nilsson
Software: G. Stenberg Wieser, M. Mihalikova, A. Bader
Visualization: G. Stenberg Wieser, H. Nilsson
Writing – original draft: G. Stenberg Wieser, M. André, H. Nilsson
Writing – review & editing: N. Edberg, M. Persson, S. Rojas Mata, H. Gunell, Y. Futaana

Abstract In the Earth's magnetosphere wave-particle interaction is a major ion energization process, playing an important role for the atmospheric escape. A common type of ion heating is associated with low-frequency broadband electric wave fields. For such waves the energy is not concentrated to a certain narrow frequency range and exhibits no peaks or dips in a power spectrum. If there are enough fluctuations close to the ion gyrofrequency the electric field may still come in resonance with gyrating ions and heat them perpendicular to the background magnetic field. We perform a proof-of-concept study to investigate if this heating mechanism may contibute significantly to the energization of planetary ions also in the induced magnetosphere of Venus. We assume Alfvénic fluctuations and estimate the electric field spectral density based on magnetic field observations. We find typical estimated electric spectral densities of a few $(mV/m)^2/Hz$ close to Venus. This corresponds to a heating rate of a few eV/s. We consider an available interaction time of ∼300 s and conclude that this mechanism could increase the energy of an oxygen ion by about a keV. Observed thermal energies are in the range 100–1,000 eV and thus, resonant wave heating may also be important at Venus.

1. Introduction

Atmospheric loss of both neutral and ionized particles to space has been observed from many different objects in the solar system: our own magnetized planet Earth, our unmagnetized planet neighbors Venus and Mars, the icy-cold dwarf planet Pluto, the moon Titan, mostly residing inside the magnetosphere of Saturn, and comets reaching small enough heliocentric distances. The escape velocities of these objects, their atmospheric constituents and temperatures, as well as their interactions with the surrounding space environment differ, making different escape processes important at various objects and also at different times during the evolution of their atmospheres (e.g., Brain et al., 2017; N. Edberg et al., 2011; Lammer et al., 2008).

Venus is an Earth-sized planet with a mean radius (R_V) of 6,052 km and an escape velocity of about 10 km/s. Its atmosphere is dominated by CO_2, and much more massive than the Earth's atmosphere, resulting in a surface pressure 90 times larger (Taylor et al., 2018). The lack of a global intrinsic magnetic field leads to the formation of a so-called induced magnetosphere (Luhmann, 1986). The constantly varying solar wind carrying the inter-planetary magnetic field (IMF) generates ionospheric currents and thereby an induced magnetic field acting to exclude the external interplanetary field. The resulting (combined) magnetic field forms a magnetic barrier of piled up fields on the dayside, a draping of the field lines around the obstacle and an elongated magnetotail on the nightside (Futaana et al., 2017).

Venus' induced magnetosphere is much smaller compared to a magnetosphere formed around a magnetized planet such as Earth. The subsolar distance to the bow shock is in the range 1.2–1.5 R_V (Whittaker et al., 2010) and the induced magnetosphere boundary (which is the analog of the magnetopause at Earth) is located at about 1.1 R_V, measured from the center of the planet (Martinecz et al., 2009). A significant amount of exospheric particles are therefore located outside these boundaries, which enables certain escape processes. Above the exobase, where collisions between atmospheric particles become less important, the dominating neutral gases are oxygen (O), helium (He) and hydrogen (H). At this altitude O^+ is the dominant heavy ion (Fox, 2004), together with nitric oxide ions according to some models (Gröller et al., 2012), and H^+ is the most abundant light ion. Oxygen and hydrogen are also the species which constitute the majority of the atmospheric loss from Venus through a number of escape processes (Brain et al., 2017; Futaana et al., 2017).

The thermal escape from Venus is negligible: its gravity is large enough and the exospheric temperature low enough to prevent even hydrogen from escaping (Lammer et al., 2006). The neutral loss occurs instead due to a series of photo-chemical reactions, which produce hot hydrogen atoms with energies above the escape energy. Modeling give a loss rate of $3.8{\cdot}10^{25}$ hydrogen atoms/s (Lammer et al., 2006).

Part of the upper atmosphere is ionized. Ions constitute a separate escape path as they can be effectively energized to escape velocities by electric fields. The solar wind convection electric field, $\vec{E}_{SW} = -\vec{v}_{SW} \times \vec{B}_{SW}$, where $\vec{v}_{SW}$ and $\vec{B}_{SW}$ are the solar wind velocity and magnetic field, accelerates exospheric ions outside of the induced magnetosphere, upstream of the bow shock and in the magnetosheath. The gyroradii of the accelerated ions are comparable to the size of the planet and some of the planetary ions originating from upstream of the obstacle reenter the induced magnetosphere and precipitate onto the upper atmosphere. The precipitating energy flux is negligible but the ions may cause loss of neutral oxygen in a sputtering process (Luhmann & Kozyra, 1991). The importance of this process is still unknown and the neutral oxygen loss often ignored.

Regions with strongly curved magnetic fields arise above the poles close to the terminator and in the magnetotail. Hall electric fields, $\vec{E}_H = \frac{1}{n_e e}\vec{j} \times \vec{B}$, where $\vec{j}$ and $\vec{B}$ are the local current density and magnetic field, and n_e and e the electron density and elementary charge, accelerate ions in these regions. A polarization (ambipolar) electric field can also develop parallel to the magnetic field. Such a field is usually attributed to an electron pressure gradient, $\vec{E}_P = -\frac{1}{n_e e}\nabla p_e$, where p_e is the electron pressure (Brain et al., 2017; Futaana et al., 2017). However, at Venus the observed parallel electric fields appear to be larger than the electron pressure gradients would yield (G. Collinson et al., 2019; G. A. Collinson et al., 2023) and additional sources for the parallel field must be sought.

The most commonly reported loss rates for O^+ are in the range $(3–6){\cdot}10^{24}$ s^{-1} (e.g., Fedorov et al., 2011; Nordström et al., 2013; Persson et al., 2018, 2020)., although higher estimates are found in the literature (e.g., Lundin, 2011). The estimated H^+ escape rates range from 1.1 up to 3.3 times the O^+ rates (Fedorov et al., 2011; Persson et al., 2018). Venus' relatively small induced magnetosphere enables the solar wind to interact directly with the upper atmosphere (Stenberg Wieser et al., 2015), and one could guess that this would yield a larger escape rate compared to a magnetized planet. However, the escape rates reported from Earth are somewhat larger than from Venus. Singly charged oxygen dominates the ion mass outflow from Earth and the average escape rate is estimated to be a few times 10^{25} s^{-1} (André, 2015, and references therein). A strong intrinsic magnetic field creates a huge magnetosphere, which prevents direct solar wind access to the atmosphere, but the big structure instead provides a larger interaction cross section to transfer solar wind energy and momentum into the magnetosphere (e.g., Gunell et al., 2018; Maggiolo et al., 2022). This can lead to a larger ion energization and atmospheric escape.

The morphology of an induced magnetosphere is governed by the direction of the IMF. A sudden change in the magnetic field direction, for example, due to a heliospheric current sheet associated with a co-rotation interaction region, causes a reconfiguration of the entire magnetosphere, which is proposed to lead to plasma loss due to magnetic reconnection events (Vech et al., 2016). N. J. T. Edberg et al. (2011) find that the ion escape from Venus increases by a factor of 1.9 during times when a corotation interaction region (CIR) or an interplanetary coronal mass ejection (ICME) impact on the planet. They suggested that the polarity change of the IMF associated with the CIR/ICME could ignite a reconnection process leading to enhanced outflow. Dimmock et al. (2018) compare results from a hybrid model with observations and confirm an increased escape of oxygen ions (of about 30%) during the passage of ICMEs. They also note a high wave activity during the ICME impact event they studied. Similarly H. Zhang et al. (2022) found significantly increased ion escape from Earth during an ICME, driven primarily by dispersive Alfvén waves interacting with the ions.

Boundary layer instabilities and other forms of wave-particle interaction are reported as additional processes believed to contribute to plasma loss, but are not very extensively investigated. Recently, however, there has been a renewed interest in Venus wave field environment and how it couples to the plasma. The Kelvin-Helmholtz instability has long been proposed to operate at the ionospheric boundary (e.g., Amerstorfer et al., 2007) and the rippled ionosphere boundary detected is indeed shown to be a consequence of this instability (Chong et al., 2018). Bader et al. (2019) showed that observed proton temperature anisotropies could explain measured mirror mode waves in the near-subsolar magnetosheath. Fränz et al. (2017) used MHD-theory to classify the observed ultra low frequency (ULF) waves around Venus and concluded that Alfvénic waves were clearly

dominant, while Jarvinen et al. (2020) used a hybrid model to show that ULF waves generated in the foreshock are able to pass through the bow shock and also to modulate the escape rate of O^+ ions.

In the absence of a direct interaction between the ionosphere and the solar wind, wave-particle interaction has been identified as a major ion energization process at Earth. Several wave modes at different frequencies are able to heat ions (André & Yau, 1997). A common type of ion heating is associated with low-frequency broadband electric wave fields (André et al., 1998). The spectral density of such broadband waves does not exhibit a peak or dip at a certain frequency but the wave power available at the ion gyrofrequency may nevertheless efficiently energize the ions (Chang et al., 1986). At Earth this heating mechanism is definitely effective and important (André et al., 1998; Nilsson et al., 2012), and it has been suggested to be important at Mars as well (Ergun et al., 2006; Fowler et al., 2017).

In this paper we investigate if ions originating from the Venusian ionosphere can be energized by the same wave heating mechanism that has been tested and verified to energize ions from the Earth's ionosphere in large regions of the terrestrial magnetosphere.

2. Theory

Electromagnetic waves with a left hand electric field component may come in or near resonance with gyrating ions. This happens if there are electric fluctuations in the vicinity of the ion gyrofrequency in the ion reference frame. If the frequency spectrum of the electric fluctuations is relatively smooth around the ion gyrofrequency one may assume that the resonance time of ions and the waves is limited by the coherence time of the electric field (Chang et al., 1986). Under these assumptions the heating rate (Chang et al., 1986) is given by

$$\frac{dW}{dt} = S_{EL} q^2 (2m)^{-1} \tag{1}$$

where S_{EL} is the spectral density of the electric field at the ion gyrofrequency due to left-hand polarized waves, and q and m are the charge and mass of the ion. The lower the coherence time of the waves is, the larger is the part of the frequency spectrum which will contribute to net heating of the ions. The theory can thus be expected to provide the right order of magnitude of the heating rate also for low coherence or varying conditions along the ion flight path. This heating mechanism results in ion energization perpendicular to the background magnetic field. Further wave-particle interaction and motion in an inhomogeneous magnetic field then spreads out the ions in pitch angle. It should be noted that this mechanism requires left-hand polarized waves. Hence, electrostatic waves, which are linearly polarized, cannot contribute to ion heating this way.

The duration of the heating determines the total ion energization and is limited by the time it takes a typical ion to pass through the region where wave-particle interaction occurs. An order of magnitude estimate can be obtained using the average ion bulk flow speed and the size of the region where the electric spectral density is significant. Given the uncertainties of the heating rate in this study, it is not worthwhile to attempt more refined methods for duration estimates.

3. Data Sets

The data used in this paper are recorded by Venus Express (VEX) (Svedhem et al., 2007), in orbit around Venus from 2006 to 2014. VEX carried a comprehensive plasma instrument suite, including ion and electron sensors as well as a magnetometer. The magnetometer (MAG; T. Zhang et al., 2006) measures the magnetic field vector with a varying sampling rate (up to 128 Hz) but the data set utilized here is resampled to 1 Hz. The plasma data is taken from the Ion Mass Analyzer (IMA; Barabash et al., 2007). For this study we only used computed moments, that is, calculated density, bulk velocity and temperature for heavy ions (assumed to be O^+). The moments are available with a time resolution of 192 s.

Due to the limited size of Venus' induced magnetosphere together with the high speed of the spacecraft close to the planet and the relatively low time resolution of the ion mass spectrometer, we will focus on the average properties in a statistical study.

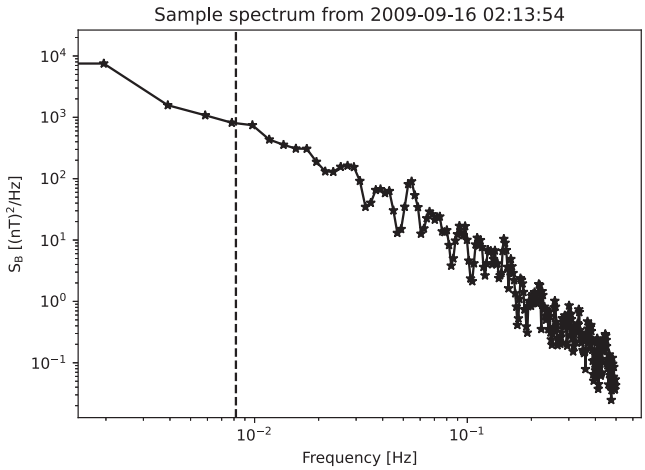

Figure 1. A sample estimate of the magnetic power spectral density $\left((nT)^2/Hz\right)$ as a function of frequency (Hz) using 512 data points as the basic record length and 1,024 data points in total, starting from 16 September 2009 at 02:13:54 UTC. The dashed vertical line indicates the O^+ gyro frequency. In Figure 2 the red line in the upper panel shows where the data points used for this spectrum are measured. It is obvious that each spectrum is an average of a large region of space, especially close to the planet where the spacecraft velocity is higher.

4. Method

The computation of the heating rate requires an estimate of the electric field power spectral density (Equation 1). There is no instrument on Venus Express measuring the electric field and therefore we base our study on the magnetic field observations. We perform a proof-of-concept study to investigate if an ion heating mechanism well established to be important around Earth also can be important around Venus. This mechanism is based on resonant heating by electric field waves around the ion gyrofrequency. Similar to Earth, Alfvén waves are likely to be common around Venus (Fränz et al., 2017; Jarvinen et al., 2020). We therefore assume the fluctuations we record are Alfvénic and that the electric and magnetic fields are related through the Alfvén speed. We later discuss that only some fraction of the observed waves need to be in resonance with the ions.

The magnetic power spectral density (used to estimate the electric power spectral density) needs to be computed with a frequency resolution that gives us a good estimate at the oxygen gyrofrequency. At the same time a finer resolution in frequency means longer record lengths and an associated coarser temporal (and thereby spatial) resolution which should be avoided. For the computations in this paper we use a basic record length in our fast Fourier transforms of 512 points, leading to a frequency bin width of $\Delta f = \sim 0.002$ Hz. The oxygen gyrofrequency in the region of interest is typically 0.005–0.02 Hz. Each estimate of the power spectral density is an average of five 512 points long records, shifted 128 points with respect to each other. Hence, 1,024 points are used for each estimate, which close to the planet (where the spacecraft velocity reaches almost 10 km/s) corresponds to a spatial scale of $\sim$1.65 R_V. The gyrofrequency is computed using the mean of the total magnetic field observed during the 1,024 points used for the power spectrum. The data records used for consecutive estimates are shifted 512 points with respect to each other and hence have a 50% overlap. To include a power spectral density estimate in the study we also demand that the oxygen gyrofrequency is larger than 1.5 Δf to make sure our frequency resolution is sufficient.

Figure 1 shows an example of the calculated magnetic power spectral density, S_B, as a function of frequency. The vertical dashed line marks the oxygen gyrofrequency, computed with the mean magnetic field strength recorded during the time period used for the corresponding S_B estimate. It should be noted that there is no peak (or other feature) at, or close to, the gyrofrequency. This is the most common situation and the figure shows a very typical spectrum. The wave field can still heat the ions using the wave power present in the vicinity of the gyrofrequency, as was described in Section 2.

The estimated spectral density of the electric field is given by $S_E = v_A^2 S_B$, where v_A is the Alfvén speed. The Alfvén speed depends on the total magnetic field and the mass density (ρ). We compute ρ using the number densities of protons and heavy ions (assuming all heavy ions are oxygen) for all times when the number of detected counts is sufficient for a reliable moment calculation. The basic time resolution of ρ is 192 s. We then interpolate ρ to the timeline of the magnetic field observation and compute v_A, whenever possible. To get v_A corresponding to a power spectrum we average all available values during the time period used to compute S_B, ignoring all missing values.

The power spectral density may vary considerably both in time and in space. We therefore make a spatial map and compute a median value at different locations. We use the Venus Solar Orbital (VSO) reference frame and bin the physical space around Venus. In VSO x_{VSO} points toward the sun, y_{VSO} in the anti-orbital direction and z_{VSO} completes a right-handed system. In this proof-of-concept study We assume cylindrical symmetry and let $R_{VSO} = \sqrt{y_{VSO}^2 + z_{VSO}^2}$. The size of a spatial bin is 0.1 × 0.1 R_V.

For each estimate of the spectral density the resulting value is assigned to all the spatial bins traversed by the spacecraft during the time data were recorded. Hence, close to the planet the same estimate may end up in up to 17 different spatial bins. For each spatial bin a histogram of all contributing spectral densities is constructed and used to obtain an estimate of the true median. As the histogram has a finite resolution (see an example in Figure 3) the

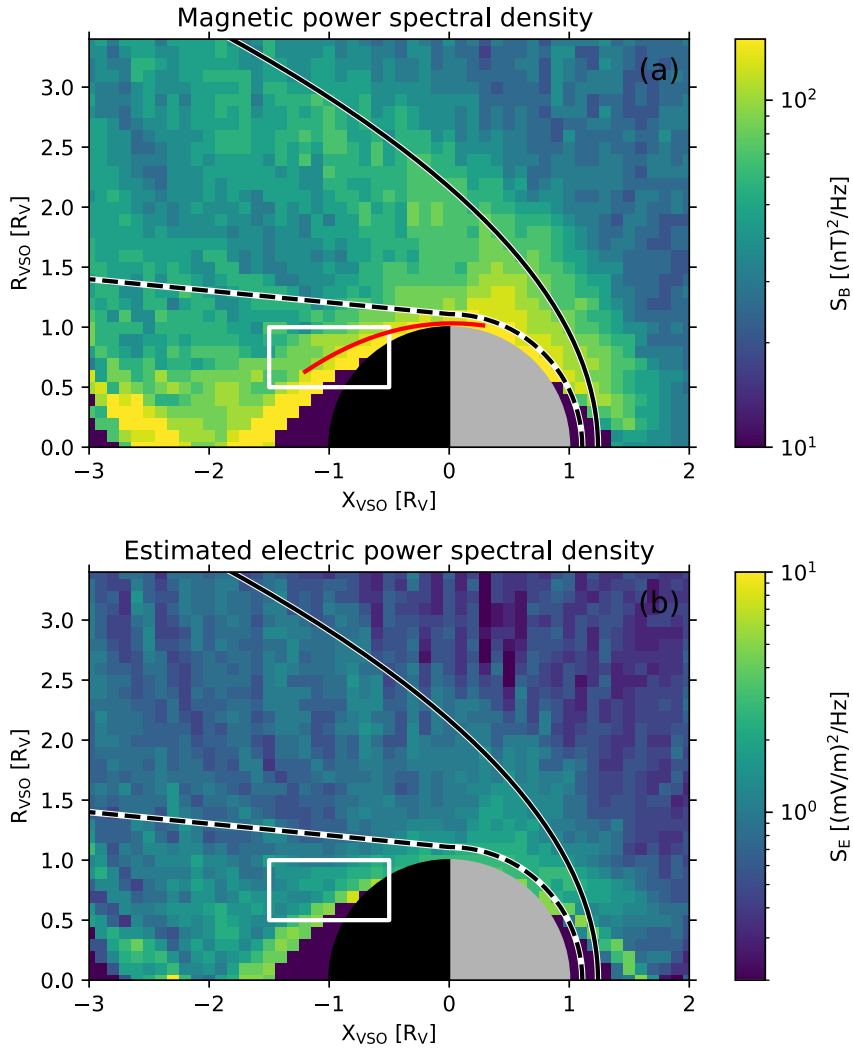

Figure 2. The top panel (a) shows a map of the median power spectral density of the magnetic field at the oxygen gyrofrequency for the period 2007–2014. The coordinate system used is Venus Solar Orbital (see text) and cylindrical symmetry is assumed. The red line shows where the data used to produce the power spectral density estimate shown in Figure 1 are recorded. The bottom panel (b) shows the median power spectral density of the estimated electric field at the oxygen gyrofrequency for the same period. See text for how the median is defined in these cases. The white box in both panels is our selected region of interest. The solid and dashed black lines show models of the bow shock (Whittaker et al., 2010) and the ion composition boundary (Martinecz et al., 2008), respectively.

estimated median can differ slightly from the true median. As we are after typical values rather than precise ones this does not matter. The median gives a smoother and more representative map than mean values, which for some bins are dominated by the extreme values. The effect of a possible Doppler shift of the waves is discussed in Section 6.

To calculate the possible energization and judge whether wave-particle interaction is important, we use the available ion moments (bulk velocity and thermal velocity) to construct spatial maps using the same reference frame as for the spectral densities, that is, VSO. For the maps of the bulk and thermal velocities we use spatial bin size of 0.2 × 0.2 R_V.

5. Results

Figure 2a shows a map of the magnetic field power spectral density at the oxygen gyrofrequency in the Venus environment. Data from the entire mission (2007–2014) are used and the solid and dashed black lines show the

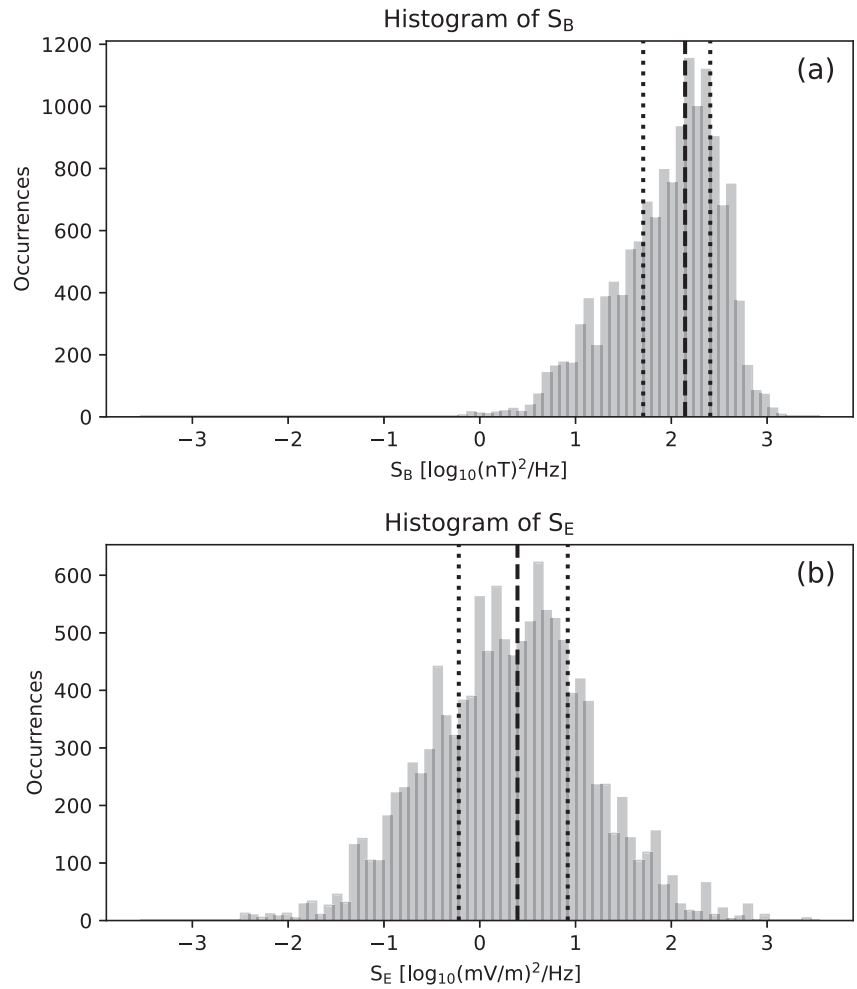

Figure 3. Upper panel (a): Histogram of the logarithm of the magnetic field spectral density at the oxygen gyrofrequency in the identified region of interest (white box in Figure 2). Bottom panel (b): Histogram of the logarithm of the estimated electric field spectral density at the oxygen gyrofrequency in the same region. The *y*-axes in the histograms show the total number of occurrences in each histogram bin. The dashed lines indicate the medians for the two histograms while the dotted lines show the 25th and the 75th percentiles. The medians presented in Figure 2 were computed from such histograms.

approximate locations of the bow shock (Whittaker et al., 2010) and the ion composition boundary (Martinecz et al., 2008). The value in each bin is the estimated median of all observations in that bin. The spectral density is slightly enhanced close to the bowshock in the dayside magnetosheath. It is also larger close to the planet and in the tail. Where the background magnetic field is smaller (e.g., in the tail) the oxygen gyrofrequency is lower and the spectral density (at the gyrofrequency) typically becomes larger if the magnetic power spectrum remains similar and resembles the one shown in Figure 1.

Figure 2b shows the spatial distribution of the estimated electric field power spectral density at the oxygen gyrofrequency. The estimated electric field power was calculated assuming Alfvén waves as described in Section 4, and the power spectral density distribution is similar to that seen for the fluctuations in the magnetic field. A typical value close to the planet is a few $(\mathrm{mV/m})^2/\mathrm{Hz}$.

To judge if the wave fields could play an important role for ion heating and escape, we focus on the power spectral densities in regions where the density of atmospheric ions is high. We therefore have picked out observations from a spatial box in the tail close to the planet, indicated by a white box in Figure 2. The distribution of the observed power spectral densities in the bins inside this box are shown as histograms for the magnetic and estimated electric fields in Figure 3. For each distribution the median is marked with a dashed line whereas the

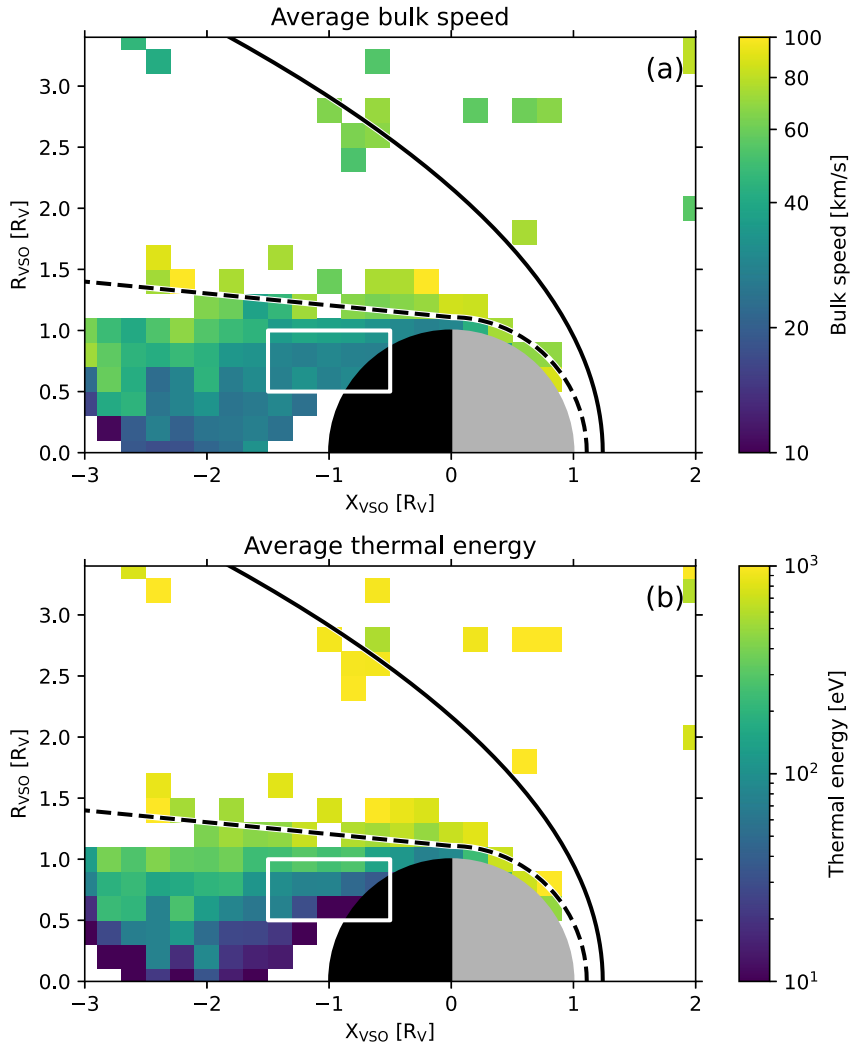

Figure 4. Upper panel (a): Average oxygen bulk velocity in the vicinity of Venus. Bottom panel (b): Average oxygen thermal energy in the vicinity of Venus. In both panels only bins with an average oxygen density larger than 0.1 cm^{-3} are shown and the bin size here is 0.2 R_V.

25th and 75th percentiles are indicated with dotted lines. The magnetic spectral density is typically 50–250 nT^2/Hz (top panel) while the estimated electric field power spectral density is typically of the order 0.5–10 $(mV/m)^2/Hz$ (bottom panel). It can be noted that the estimated electric power spectral density quite often reaches 10 $(mV/m)^2/Hz$ and can at times be as high as 100 $(mV/m)^2/Hz$.

The net heating rates obtained from the estimated observed electric field spectral densities can now be estimated from Equation 1 giving $dW/dt = 1.5 - 30$ eV/s for estimated electric spectral densities of 0.5–10$(mV/m)^2/Hz$. The previous statement assumes that 100% of the wave activity can be used to heat the ions. This would correspond to only (incoherent) lefthand circularly polarized waves at the gyro frequency. A more realistic upper limit is linearly polarized waves, giving 50% efficiency. In the following we will use 30%, as further discussed in Section 7.

To get the total heating (energy increase), ΔW, we need to estimate the time, T, during which the heating occurs. With the obtained heating rate, dW/dt, we then get $\Delta W = T \cdot dW/dt$. In Figure 4 the average oxygen bulk and thermal velocities during the Venus Express mission are shown. As we are interested in the heating of planetary ions, only bins where the average oxygen ion density is larger than 0.1 cm^{-3} are shown. Focusing on the same region close to the planet as previously (white box) we note that the typical bulk velocity is ≈30 km/s while the

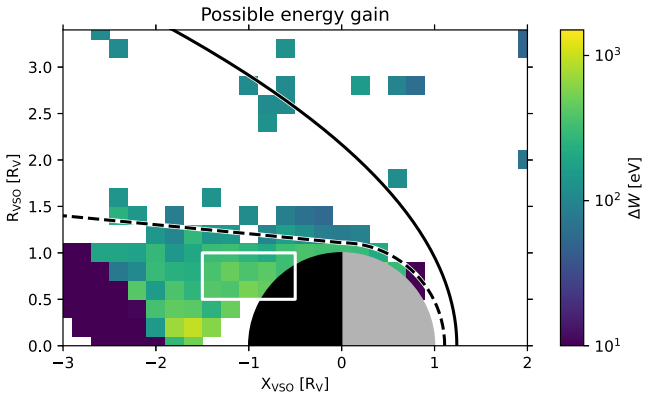

Figure 5. Potential energy gain of oxygen ions in the vicinity of Venus, assuming 30% of the available wave energy can be used and that the interaction region everywhere has the size of 10,000 km.

thermal energy is below 100 eV (≈30 km/s). Assuming the size of the heating region to be 10,000 km (similar to the size of the planet) and using the bulk speed 30 km/s gives ∼300 s as a typical interaction time. For an order of magnitude estimate we use a spectral density of 4 $(\mathrm{mV/m})^2/\mathrm{Hz}$ and take 30% of this which gives a heating rate of about 3 eV/s. This results in a typical O^+ energy increase of $\Delta W = T \cdot dW/dt \approx 300\ s \cdot 3\ \mathrm{eV/s} \approx 1\ \mathrm{keV}$.

Figure 5 shows a map of the potential energy increase, applying the same calculation as above for each spatial bin. The bulk speeds are found from Figure 4 and the size of the interaction region is kept 10,000 km. The estimated electric power spectral densities (from Figure 2) are originally computed with a higher spatial resolution and are averaged over four bins.

The waves could in principle transfer 1 keV to the ion during the interaction. Ions in the ionosphere are cold (few eV) but from the map of the oxygen thermal energy (Figure 4b) we note that the thermal energies increase further away from the planet. In the white box the average energy is around 100 eV but even further away the oxygen thermal energy can reach a keV. Hence, the estimated energization corresponds to typical thermal energies of the oxygen ions we observe. We therefore conclude that heating by Alfvén waves may indeed contribute significantly to the energization of planetary ions around Venus.

6. Doppler Shift Considerations

Our analysis considers waves at the local oxygen gyrofrequency. The waves observed on the spacecraft may, however, be Doppler shifted. The frequency in the plasma reference frame differs from the observed (angular) frequency by $\Delta\omega = v \cdot k = v_\perp \cdot k_\perp + v_\parallel \cdot k_\parallel$, where $v_\perp$ and $k_\perp$ ($v_\parallel$ and $k_\parallel$) are the plasma velocity and the wave vector components perpendicular (parallel) to the background magnetic field. If the Doppler shift is too large the chosen approach would not give a good estimate of the spectral density at the gyrofrequency.

To estimate the possible Doppler shift we set $v_\parallel = v_\perp = 30$ km/s, which is the typical bulk velocity in the region close to the planet we considered above. By doing so we are overestimating at least one of the velocity components but it is good enough for a rough estimate. The parallel wave vector $(k_\parallel)$ is given from the assumption of Alfvén waves, that is, $k_\parallel = \omega_{cO^+}/v_A$, where ω_{cO^+} is the oxygen (angular) gyrofrequency and v_A the Alfvén velocity. The Alfvén velocity is about 100 km/s close to Venus (not shown) and for a magnetic field of 10 nT we get $\omega_{cO^+} = 0.06$ rad/s (=0.010 Hz) and $k_\parallel = 0.06 \cdot 10^{-6}\ \mathrm{m}^{-1}$. The perpendicular wave vector $(k_\perp)$ is obtained by setting $k_\perp \cdot r_{O^+} = 1$, where r_{O^+} is the oxygen gyroradius. For larger perpendicular wavelengths we assume the wave would be heavily damped (André, 1985). With a thermal velocity of 30 km/s and a magnetic field of 10 nT we get $r_{O^+} = 500$ km and $k_\perp = 2 \cdot 10^{-6}\ \mathrm{m}^{-1}$.

The total (maximum) Doppler shift is then $\Delta\omega \approx 0.08$ rad/s (= 0.012 Hz), which is similar to the typical oxygen gyrofrequency. The actual Doppler shift will vary and most often be smaller than our estimate. Conferring Figure 1 we then note that a Doppler shift in the very extreme case could change the power spectral density estimate by a factor of 10, but the effect is typically smaller and we believe our power spectral density estimates are still valid.

In principle, quasi-static structures in the plasma frame could be Doppler shifted and observed at the oxygen gyrofrequency in the spacecraft frame. However, it is not likely that the broadband spectra we observe are only resulting from static structures. There are certainly some time variations in the plasma frame at this frequency. We use the same approach as in the near Earth case when both the electric and magnetic broadband spectra are observed, for example, (André et al., 1998; Waara et al., 2011) and investigate how large fraction of the waves observed in the spacecraft frame are needed to explain the observed ion energies.

7. Discussion

We have performed a feasibility study to see if ion energization by waves around the ion gyrofrequency can be important for energization and subsequent outflow of O^+ ions from the ionosphere of Venus. This is the same

mechanism that has been verified to be important in several regions in the Earth's magnetosphere. Early studies investigated energization in the central plasma sheet (Chang et al., 1986; Retterer et al., 1987), the auroral region (André et al., 1988) and the polar cusp and cleft (André et al., 1990). Later the Cluster mission allowed for similar studies over a vast range of altitudes and regions, as for the mid altitude cusp (Bouhram et al., 2003), the high altitude cusp (Waara et al., 2011, 2012) and for the high altitude cusp, mantle and polar cap (Nilsson et al., 2012, 2013).

In all these studies, a varying fraction of the estimated electric field power spectral density near the ion gyrofrequency needs to be in resonance with the ions to explain the observed ion energies. Typically a larger fraction (25%–45%) of the estimated electric power spectral density is needed for higher energies (a few keV) at high altitudes (Slapak et al., 2011; Waara et al., 2011), in regions with a relatively high plasma beta, that is, in the cusp and mantle. At lower altitudes and lower ion energies (~100 eV) the fraction of the observed wave spectral density needed to explain observations is smaller, on the order of 1%. Here most of the spectral density observed at the gyrofrequency is due to waves not in resonance with the ions, including Doppler shifted quasi-static structures. Given the weaker magnetic field at Venus, it seems plausible to assume that the situation is more similar to what is observed at high altitude at Earth, that is, a fraction of about 30%, which is what we assume in our estimates of the heating rate. A difference from Earth is that we do not observe the spatial correlation on planetary scale between the oxygen thermal energy and the estimated electric power spectral density observed at Earth (Nilsson et al., 2012). The thermal energy map at Venus does resemble what is seen at Earth but the power spectral density map is different. In Figure 2 we note an increase of the spectral density in the nightside ionosphere. Here it must be noted that our spatial resolution of the spectral density estimates is very coarse, and the method used smears out the spectral density along the spacecraft orbit. Our approach does not allow us to investigate if the wave activity is concentrated to certain regions or times. We only conclude that observed properties of the region of interest indicate that resonant heating is a plausible energization mechanism.

It should be noted that what we present are median values of the spectral density. These values are high enough to cause significant oxygen energization almost all the time. Hence, the resonant heating mechanism may often play an important role, not just during times with special conditions resulting in increased wave activity. That said, our estimates are likely slightly higher than the true values. The densities we use are likely too low, as the field of view of the spectrometer is limited and the spacecraft itself also blocks ions traveling from certain directions and the full ion distribution may not always be observed. This leads to an overestimate of the Alfvén velocity used to compute the estimated electric power spectral density. As we are only investigating the feasibility of the resonant ion heating mechanism this does not matter so much. From the histogram in Figure 3b we see that the spectral density will often be high enough to cause a significant heating even if the density is underestimated by a factor of 5.

To obtain the estimated electric power spectral density when only measurements of the wave magnetic field are available, we assume the waves to be linear Alfvén waves with phase velocity v_A and the plasma to be homogeneous. We then consider the observed broadband (in frequency) power spectral density of the magnetic field (S_B) around the ion gyrofrequency, use v_A to estimate the electric spectral density S_E and use this spectral density to estimate the heating rate. Should the waves strictly fulfill the assumptions of linear waves in a homogeneous plasma, there would be lefthand waves with phase velocity v_A only well below the ion gyrofrequency, and no such waves exactly at the gyrofrequency (e.g., André, 1985). However, Doppler shifts can be significant as discussed above, and non-linear effects can broaden the spectrum (e.g., Klatt et al., 2005; Wahlund et al., 1994). Wave spectra associated with ion energization near Earth are typically broadband for both S_E and S_B (e.g., André et al., 1988; André et al., 1990, 1998; Waara et al., 2011). Thus it is reasonable to use broadband S_B spectra at Venus to obtain broadband S_E spectra used to estimate ion energization.

Energization by waves around the ion gyrofrequency has been considered also at Mars by Ergun et al. (2006). They noted that for the mechanism to be effective they needed to assume a high efficiency in the heating, assuming 50% of the observed or estimated spectral density at the gyrofrequency were due to lefthand polarized waves heating the ions. Similarly Fowler et al. (2018) assumed that all wave energy in magnetosonic waves propagating down to the ionosphere was used up in ion heating. Hence, even if the importance of this resonant energization mechanism at different solar system objects needs to be further investigated, it likely plays a role not only at Earth but at many other places in the solar system.

8. Conclusions and Outlook

We estimated the electric power spectral density close to the oxygen gyro frequency in the vicinity of Venus to be in the range a few (0.5–10) $mV/m^2/Hz$. If 30% of the wave energy can be used for resonant heating of the oxygen ions we get heating rates of typically a few eV/s. This is enough for the ions to gain up to 1 keV during an estimated interaction time of 300 s. The oxygen ions seen also have thermal energies in the range 100 eV to 1 keV. We conclude that heating of planetary ions (O^+) by waves near the ion gyrofrequency is a feasible mechanism at Venus, which may explain ion energies up to about a keV and associated ionospheric outflow.

Our study illuminates the importance of including high resolution plasma wave and particle instrumentation on future Venus missions. With no such mission in the near future, there is still the opportunity to use data taken by spacecraft making close flybys of the planet, such as Bepi-Colombo or Parker Solar Probe. Case studies based on such observations would definitely contribute to the understanding of the importance of resonant ion heating at our sister planet.

Venus serves as an analog for close-in exoplanets and the discovery of thousands of worlds orbiting other stars strongly poses the question about habitability and the presence of life elsewhere in the universe. One of the keys in order to judge the possibilities for life to emerge is to understand the evolution of planetary atmospheres and the effect over time of atmospheric escape to space (Owen, 2019). If ion energization by resonant waves is important for escape processes at planets both with and without an intrinsic magnetic field in our solar system; it seems likely that the same mechanism is important at many exoplanets.

Data Availability Statement

The Venus Express data used in this study is available through the ESA Planetary Science Archive (ESA PSA) at https://archives.esac.esa.int/psa/ftp/VENUS-EXPRESS/ASPERA4. Additional ASPERA-4 high-level data provided by the Swedish Institute of Space Physics data archive is available at https://irfpy.irf.se/pub/data/aspera4. Data analysis was done using NumPy version 1.26.4 (Harris et al., 2020). Figures were made using Matplotlib version 3.5.2 (Caswell et al., 2021; Hunter, 2007) available under the Matplotlib license at https://matplotlib.org/.

Acknowledgments
The authors acknowledge the Principal Investigators T. Zhang (OAW, Graz) and Yoshifumi Futaana (IRF, Kiruna, Sweden) of the MAG and ASPERA-4 instruments onboard the Venus Express mission. The high-level data of ASPERA-4 on Venus Express was produced by Swedish Institute of Space Physics (IRF), co-funded by the Swedish National Space Agency (Dnr 79/19). We acknowledge all the efforts at IRF, led by the Principle Investigator Yoshifumi Futaana.

References

Amerstorfer, U. V., Erkaev, N. V., Langmayr, D., & Biernat, H. K. (2007). On Kelvin–Helmholtz instability due to the solar wind interaction with unmagnetized planets. *Planetary and Space Science*, *55*(12), 1811–1816. https://doi.org/10.1016/j.pss.2007.01.015

André, M. (1985). Dispersion surfaces. *Journal of Plasma Physics*, *33*, 1–19. https://doi.org/10.1017/s0022377800002270

André, M. (2015). Previously hidden low-energy ions: A better map of near-earth space and the terrestrial mass balance. *Physica Scripta*, *90*(12), 128005. https://doi.org/10.1088/0031-8949/90/12/128005

André, M., Crew, G. B., Peterson, W. K., Persoon, A. M., Pollock, C. J., & Engebretson, M. J. (1990). Ion heating by broadband low-frequency waves in the cusp/cleft. *Journal of Geophysical Research*, *95*(A12), 20809–20823. https://doi.org/10.1029/JA095iA12p20809

André, M., Matson, L., Koskien, H., & Erlandson, R. (1988). Local transverse ion energization in and near the polar cusp. *Geophysical Research Letters*, *15*(1), 107–110. https://doi.org/10.1029/GL015i001p00107

André, M., Norqvist, P., Andersson, L., Eliasson, L., Eriksson, A. I., Blomberg, L., et al. (1998). Ion energization mechanisms at 1700 km in the auroral region. *Journal of Geophysical Research*, *103*(A3), 4199–4222. https://doi.org/10.1029/97JA00855

André, M., & Yau, A. (1997). Theories and observations of ion energization and outflow in the high latitude magnetosphere. *Space Science Reviews*, *80*(1), 27–48. https://doi.org/10.1023/A:1004921619885

Bader, A., Stenberg Wieser, G., André, M., Wieser, M., Futaana, Y., Persson, M., et al. (2019). Proton temperature anisotropies in the plasma environment of Venus. *Journal of Geophysical Research: Space Physics*, *124*(5), 3312–3330. https://doi.org/10.1029/2019JA026619

Barabash, S., Sauvaud, J.-A., Gunell, H., Andersson, H., Grigoriev, A., Brinkfeldt, K., et al. (2007). The analyser of space plasmas and energetic atoms (ASPERA-4) for the Venus express mission. *Planetary and Space Science*, *55*(12), 1772–1792. https://doi.org/10.1016/j.pss.2007.01.014

Bouhram, M., Malingre, M., Jasperse, J. R., Dubouloz, N., & Sauvaud, J.-A. (2003). Modeling transverse heating and outflow of ionospheric ions from the dayside cusp/cleft. 2 applications. *Annales Geophysicae*, *21*(8), 1773–1791. https://doi.org/10.5194/angeo-21-1773-2003

Brain, D. A., Bagenal, F., Ma, Y. J., Nilsson, H., & Stenberg Wieser, G. (2017). Atmospheric escape from unmagnetized bodies. *Journal of Geophysical Research: Planets*, *121*(12), 2364–2385. https://doi.org/10.1002/2016JE005162

Caswell, T. A., Lee, M. D. A., de Andrade, E. S., Hunter, J., Hoffmann, T., Firing, E., et al. (2021). matplotlib/matplotlib: REL: V3.4.1 [Software]. https://doi.org/10.5281/zenodo.4649959

Chang, T., Crew, G. B., Hershkowitz, N., Jasperse, J. R., Retterer, J. M., & Winningham, J. D. (1986). Transverse acceleration of oxygen ions by electromagnetic ion cyclotron resonance with broad band left-hand polarized waves. *Geophysical Research Letters*, *13*(7), 636–639. https://doi.org/10.1029/GL013i007p00636

Chong, G. S., Pope, S. A., Walker, S. N., Frahm, R. A., Zhang, T., & Futaana, Y. (2018). A statistical study of ionospheric boundary wave formation at Venus. *Journal of Geophysical Research: Space Physics*, *123*(9), 7668–7685. https://doi.org/10.1029/2018JA025644

Collinson, G., Glocer, A., Xu, S., Mitchell, D., Frahm, R. A., Grebowsky, J., et al. (2019). Ionospheric ambipolar electric fields of mars and Venus: Comparisons between theoretical predictions and direct observations of the electric potential drop. *Geophysical Research Letters*, *46*(3), 1168–1176. https://doi.org/10.1029/2018GL080597

Collinson, G. A., Frahm, R. A., Glocer, A., Daldorff, L., Thiemann, E., Kang, S.-B., et al. (2023). A survey of strong electric potential drops in the ionosphere of Venus. *Geophysical Research Letters*, *50*(18), e2023GL104989. https://doi.org/10.1029/2023GL104989

Dimmock, A. P., Alho, M., Kallio, E., Pope, S. A., Zhang, T. L., Kilpua, E., et al. (2018). The response of the Venusian plasma environment to the passage of an ICME: Hybrid simulation results and Venus express observations. *Journal of Geophysical Research: Space Physics*, *123*(5), 3580–3601. https://doi.org/10.1029/2017JA024852

Edberg, N., Ågren, K., Wahlund, J.-E., Morooka, M., Andrews, D., Cowley, S., et al. (2011a). Structured ionospheric outflow during the CASSINI t55-t59 titan flybys. *Planetary and Space Science*, *59*(8), 788–797. https://doi.org/10.1016/j.pss.2011.03.007

Edberg, N. J. T., Nilsson, H., Futaana, Y., Stenberg, G., Lester, M., Cowley, S. W. H., et al. (2011b). Atmospheric erosion of Venus during stormy space weather. *Journal of Geophysical Research*, *116*(A9), A09308. https://doi.org/10.1029/2011JA016749

Ergun, R. E., Andersson, L., Peterson, W. K., Brain, D., Delory, G. T., Mitchell, D. L., et al. (2006). Role of plasma waves in Mars' atmospheric loss. *Geophysical Research Letters*, *33*(14), 14103. https://doi.org/10.1029/2006GL025785

Fedorov, A., Barabash, S., Sauvaud, J. A., Futaana, Y., Zhang, T. L., Lundin, R., & Ferrier, C. (2011). Measurements of the ion escape rates from Venus for solar minimum. *Journal of Geophysical Research*, *116*(A7), A07220. https://doi.org/10.1029/2011JA016427

Fowler, C. M., Andersson, L., Ergun, R. E., Harada, Y., Hara, T., Collinson, G., et al. (2018). Maven observations of solar wind-driven magnetosonic waves heating the Martian dayside ionosphere. *Journal of Geophysical Research: Space Physics*, *123*(5), 4129–4149. https://doi.org/10.1029/2018JA025208

Fowler, C. M., Ergun, R. E., Andersson, L., Peterson, W. K., Hara, T., Mcfadden, J., et al. (2017). Ion heating in the Martian ionosphere. *Journal of Geophysical Research: Space Physics*, *122*(10), 10612–10625. https://doi.org/10.1002/2017JA024578

Fox, J. L. (2004). Advances in the aeronomy of Venus and mars. *Advances in Space Research*, *33*(2), 132–139. https://doi.org/10.1016/j.asr.2003.08.014

Fränz, M., Echer, E., Marques de Souza, A., Dubinin, E., & Zhang, T. L. (2017). Ultra low frequency waves at Venus: Observations by the Venus express spacecraft. *Planetary and Space Science*, *146*, 55–65. https://doi.org/10.1016/j.pss.2017.08.011

Futaana, Y., Stenberg Wieser, G., Barabash, S., & Luhmann, J. G. (2017). Solar wind interaction and impact on the Venus atmosphere. *Space Science Reviews*, *212*(3), 1453–1509. https://doi.org/10.1007/s11214-017-0362-8

Gröller, H., Lammer, H., Lichtenegger, H. I. M., Pfleger, M., Dutuit, O., Shematovich, V. I., et al. (2012). Hot oxygen atoms in the Venus nightside exosphere. *Geophysical Research Letters*, *39*(3), L03202. https://doi.org/10.1029/2011GL050421

Gunell, H., Maggiolo, R., Nilsson, H., Stenberg Wieser, G., Slapak, R., Lindkvist, J., et al. (2018). Why an intrinsic magnetic field does not protect a planet against atmospheric escape. *A&*, *614*, L3. https://doi.org/10.1051/0004-6361/201832934

Harris, C. R., Millman, K. J., van der Walt, S. J., Gommers, R., Virtanen, P., Cournapeau, D., et al. (2020). Array programming with NumPy. *Nature*, *585*(7825), 357–362. https://doi.org/10.1038/s41586-020-2649-2

Hunter, J. D. (2007). Matplotlib: A 2d graphics environment. *Computing in Science & Engineering*, *9*(3), 90–95. https://doi.org/10.1109/MCSE.2007.55

Jarvinen, R., Alho, M., Kallio, E., Pulkkinen, I., & Tuija (2020). Oxygen ion escape from Venus is modulated by ultra-low frequency waves. *Geophysical Research Letters*, *47*(11), e2020GL087462. https://doi.org/10.1029/2020GL087462

Klatt, E. M., Kintner, P. M., Seyler, C. E., Liu, K., MacDonald, E. A., & Lynch, K. A. (2005). Sierra observations of Alfvénic processes in the topside auroral ionosphere. *Journal of Geophysical Research*, *110*(A10), A10S12. https://doi.org/10.1029/2004JA010883

Lammer, H., Kasting, J. F., Chassefière, E., Johnson, R. E., Kulikov, Y. N., & Tian, F. (2008). Atmospheric escape and evolution of terrestrial planets and satellites. *Space Science Reviews*, *139*(1), 399–436. https://doi.org/10.1007/s11214-008-9413-5

Lammer, H., Lichtenegger, H. I. M., Biernat, H. K., Erkaev, N. V., Arshukova, I. L., Kolb, C., et al. (2006). Loss of hydrogen and oxygen from the upper atmosphere of Venus. *Planetary and Space Science*, *54*(13), 1445–1456. https://doi.org/10.1016/j.pss.2006.04.022

Luhmann, J. G. (1986). The solar wind interaction with Venus. *Space Science Reviews*, *44*(3), 241–306. https://doi.org/10.1007/BF00200818

Luhmann, J. G., & Kozyra, J. U. (1991). Dayside pickup oxygen ion precipitation at Venus and mars: Spatial distributions, energy deposition and consequences. *Journal of Geophysical Research*, *96*(A4), 5457–5467. https://doi.org/10.1029/90JA01753

Lundin, R. (2011). Ion acceleration and outflow from mars and Venus: An overview. In K. Szego (Ed.), *The plasma environment of venus, mars, and titan* (Vol. 37, pp. 309–334). Springer. https://doi.org/10.1007/978-1-4614-3290-6_9

Maggiolo, R., Maes, L., Cessateur, G., Darrouzet, F., De Keyser, J., & Gunell, H. (2022). The earth's magnetic field enhances solar energy deposition in the upper atmosphere. *Journal of Geophysical Research: Space Physics*, *127*(12), e2022JA030899. https://doi.org/10.1029/2022JA030899

Martinecz, C., Boesswetter, A., Fränz, M., Roussos, E., Woch, J., Krupp, N., et al. (2009). Plasma environment of Venus: Comparison of Venus express ASPERA-4 measurements with 3-D hybrid simulations. *Journal of Geophysical Research*, *114*(E9), E00B30. https://doi.org/10.1029/2008JE003174

Martinecz, C., Fränz, M., Woch, J., Krupp, N., Roussos, E., Dubinin, E., et al. (2008). Location of the bow shock and ion composition boundaries at Venus—Initial determinations from Venus express ASPERA-4. *Planetary and Space Science*, *56*(6), 780–784. https://doi.org/10.1016/j.pss.2007.07.007

Nilsson, H., Barghouthi, I. A., Slapak, R., Eriksson, A. I., & André, M. (2012). Hot and cold ion outflow: Spatial distribution of ion heating. *Journal of Geophysical Research*, *117*(A11), A11201. https://doi.org/10.1029/2012JA017974

Nilsson, H., Barghouthi, I. A., Slapak, R., Eriksson, A. I., & André, M. (2013). Hot and cold ion outflow: Observations and implications for numerical models. *Journal of Geophysical Research (Space Physics)*, *118*(1), 105–117. https://doi.org/10.1029/2012JA017975

Nordström, T., Stenberg, G., Nilsson, H., Barabash, S., & Zhang, T. L. (2013). Venus ion outflow estimates at solar minimum: Influence of reference frames and disturbed solar wind conditions. *Journal of Geophysical Research: Space Physics*, *118*(6), 3592–3601. https://doi.org/10.1002/jgra.50305

Owen, J. E. (2019). Atmospheric escape and the evolution of close-in exoplanets. *Annual Review of Earth and Planetary Sciences*, *47*(1), 67–90. https://doi.org/10.1146/annurev-earth-053018-060246

Persson, M., Futaana, Y., Fedorov, A., Nilsson, H., Hamrin, M., & Barabash, S. (2018). H+/o+ escape rate ratio in the Venus magnetotail and its dependence on the solar cycle. *Geophysical Research Letters*, *45*(20), 10805–10811. https://doi.org/10.1029/2018GL079454

Persson, M., Futaana, Y., Ramstad, R., Masunaga, K., Nilsson, H., Hamrin, M., et al. (2020). The Venusian atmospheric oxygen ion escape: Extrapolation to the early solar system. *Journal of Geophysical Research: Planets*, *125*(3), e2019JE006336. https://doi.org/10.1029/2019JE006336

Retterer, J. M., Chang, T., Crew, G. B., Jasperse, J. R., & Winningham, J. D. (1987). Monte Carlo modeling of ionospheric oxygen acceleration by cyclotron resonance with broad-band electromagnetic turbulence. *Physical Review Letters*, *59*(1), 148–151. https://doi.org/10.1103/PhysRevLett.59.148

Slapak, R., Nilsson, H., Waara, M., André, M., Stenberg, G., & Barghouthi, I. A. (2011). O+ heating associated with strong wave activity in the high altitude cusp and mantle. *Annales Geophysicae*, *29*(5), 931–944. https://doi.org/10.5194/angeo-29-931-2011

Stenberg Wieser, G., Ashfaque, M., Nilsson, H., Futaana, Y., Barabash, S., Diéval, C., et al. (2015). Proton and alpha particle precipitation onto the upper atmosphere of venus. *Planetary and Space Science*, *113–114*, 369–377. https://doi.org/10.1016/j.pss.2015.01.018

Svedhem, H., Titov, D., McCoy, D., Lebreton, J.-P., Barabash, S., Bertaux, J.-L., et al. (2007). Venus express—The first European mission to Venus. *Planetary and Space Science*, *55*(12), 1636–1652. https://doi.org/10.1016/j.pss.2007.01.013

Taylor, F. W., Svedhem, H., & Head, J. W. (2018). Venus: The atmosphere, climate, surface, interior and near-space environment of an earth-like planet. *Space Science Reviews*, *214*(1), 35. https://doi.org/10.1007/s11214-018-0467-8

Vech, D., Stenberg, G., Nilsson, H., Edberg, N. J. T., Opitz, A., Szegő, K., et al. (2016). Statistical features of the global polarity reversal of the Venusian induced magnetosphere in response to the polarity change in interplanetary magnetic field. *Journal of Geophysical Research: Space Physics*, *121*(5), 3951–3962. https://doi.org/10.1002/2015JA021995

Waara, M., Nilsson, H., Slapak, R., André, M., & Stenberg, G. (2012). Oxygen ion energization by waves in the high altitude cusp and mantle. *Annales Geophysicae*, *30*(9), 1309–1314. https://doi.org/10.5194/angeo-30-1309-2012

Waara, M., Slapak, R., Nilsson, H., Stenberg, G., André, M., & Barghouthi, I. A. (2011). Statistical evidence for O+ energization and outflow caused by wave-particle interaction in the high altitude cusp and mantle. *Annales Geophysicae*, *29*(5), 945–954. https://doi.org/10.5194/angeo-29-945-2011

Wahlund, J. E., Louarn, P., Chust, T., de Feraudy, H., Roux, A., Holback, B., et al. (1994). Observations of ion acoustic fluctuations in the auroral topside ionosphere by the FREJA S/C. *Geophysical Research Letters*, *21*(17), 1835–1838. https://doi.org/10.1029/94GL01290

Whittaker, I., Guymer, G., Grande, M., Pintér, B., Barabash, S., Federov, A., et al. (2010). Venusian bow shock as seen by the ASPERA-4 ion instrument on Venus express. *Journal of Geophysical Research*, *115*(A9), A09224. https://doi.org/10.1029/2009JA014826

Zhang, H., Fu, S., Fu, S., Zhong, J., Ni, B., Wei, Y., et al. (2022). A highway for atmospheric ion escape from earth during the impact of an interplanetary coronal mass ejection. *The Astrophysical Journal*, *937*(1), 4. https://doi.org/10.3847/1538-4357/ac8a93

Zhang, T., Baumjohann, W., Delva, M., Auster, H.-U., Balogh, A., Russell, C., et al. (2006). Magnetic field investigation of the Venus plasma environment: Expected new results from Venus express. *Planetary and Space Science*, *54*(13), 1336–1343. https://doi.org/10.1016/j.pss.2006.04.018